Plastic scintillators with 1-phenyl-3-(mesityl)-2-pyrazoline as unique fluorophore for efficient neutron/gamma pulse shape discrimination

Fabrice Bisaro, Alya Inial, Jérémie Gatignol, Florent Allix, Aurélie Stallivieri, Jean-Luc Renaud, Lynda Achouri, Marian Parlog, Franck Delaunay, Thi-Nhàn Pham, et al.

Plastic scintillators with 1-phenyl-3-(mesityl)-2-pyrazoline as unique fluorophore for efficient neutron/gamma pulse shape discrimination

Fabrice Bisaro [a], Alya Inial [a], Jérémie Gatignol [a], Florent Allix [a], Aurélie Stallivieri [a], Jean-Luc Renaud [a], Lynda Achouri [b], Marian Parlog [b,c], Franck Delaunay [b], Thi-Nhàn Pham [a], Matthieu Hamel [d], Sylvain Gaillard [a]

[a] Normandie Univ, ENSICAEN, UNICAEN, CNRS, LCMT, 14000 Caen, France
[b] LPC Caen, Normandie Univ, ENSICAEN, UNICAEN, CNRS/IN2P3, 14000 Caen, France
[c] Horia Hulubei National Institute for R&D in Physics and Nuclear Ingineering (IFIN-HH), P.O.BOX MG-6, RO-76900, Bucharest Màgurele, Romania
[d] Université Paris-Saclay, CEA, List, Laboratoire Capteurs et Architectures Électroniques, F-91120 Palaiseau, France

Abstract

The development of highly efficient plastic scintillators for neutron/gamma pulse shape discrimination is a matter of current interest. This is generally achieved using two fluorophores, with one of them being added to the polymer formulation at a concentration higher than typically 15 weight percent (wt%). Here, we report our results concerning the development of highly performant poly(vinyltoluene)-based (PVT) plastic scintillators for efficient fast neutron/gamma pulse shape discrimination, using 1-phenyl-3-(mesityl)-2-pyrazoline (**1**) as the only guest fluorophore. On our route during this study, the synthesis of the compound **1** has been revisited. Analysis and evaluation of the radioluminescence properties of these novel PVT-based plastic scintillators containing compound **1** are also described. In particular their light output and neutron/gamma discrimination ability were characterized. The sample doped with 15 wt% of compound **1** has a light output of 0.65 relative to EJ-200 and a neutron/gamma discrimination figure of merit of 0.84 in the range 450–500 keVee.

Keywords

Neutron/gamma discrimination, Plastic scintillators, Polymers, Fluorophores, Pyrazolines

1. Introduction

Detection of fast neutrons (i.e. neutrons with kinetic energies of a few hundred keV or higher) in the presence of a gamma-ray background has been a topic of interest for decades for fundamental nuclear physics studies or applications. Current interests are the radiation protection of individuals working in nuclear facilities and the limitation or blocking of illegal traffics of special nuclear materials like $^{233/235}$U and ^{239}Pu, the latter being potentially used for the production of nuclear weapons. Tremendous progress has been made in this research field with the development of a wide range of efficient scintillators, including organic (single crystals [1], liquids [2], plastics [3], glasses [4]) and inorganic scintillators (single crystals [5], gases [6]).

To date, liquid scintillators are the best trade-off in terms of detection efficiency, neutron/gamma discrimination performance and overall cost [7]. One of the major drawbacks of liquid scintillators is that they rely on the use of toxic and/or flammable aromatic solvents. Even if these drawbacks can be reduced by the use of linear alkylbenzene (LAB) [8] or diisopropylnaphthalene (DIN) [9] as solvent, potential leaks from the container and thermal expansion, which is highly temperature dependent, can strongly limit outdoor applications. Another disadvantage of liquid scintillators is their need to be in an inert environment as oxygen will quench the delayed fluorescence, largely responsible for the Pulse Shape Discrimination (PSD) capability.

Whereas the use of plastic scintillators seems an appealing alternative to palliate these limitations, they were for long neglected for a large-scale use due to their lack of efficiency for neutron/gamma PSD.

Since the seminal development by Brooks et al. in 1960 [10], 50 years had passed, until Zaitseva et al., in 2012, developed new plastic scintillators with efficient neutron/gamma PSD [11]. The development of plastic scintillators has then become one of the most exciting and challenging subjects in this research field [12].

Briefly, neutron/gamma discrimination relies on the fact that the time profile of the intensity of the scintillation pulse (the "pulse shape") depends on the nature of the exciting particle. More precisely, under neutron and gamma radiations, two fluorescence mechanisms occur, whose respective emissions differ in their time scales.

Prompt fluorescence is emitted by molecules directly excited in their singlet states, while ionization followed by recombination mainly excites triplet states that can lead to delayed fluorescence through the following mechanism. When two triplet states are close enough, they can undergo a "triplet–triplet annihilation", giving one molecule in its ground state and the other one in its first singlet state. The latter ultimately deexcites, thus giving delayed fluorescence. The intensity and time scale of this delayed component are limited by the triplet–triplet annihilation probability. Gamma-ray interactions within the material produce electrons that excite molecules with a low density thus favouring prompt fluorescence, whereas fast neutrons generate recoil protons that produce a higher excitation density, increasing the triplet–triplet annihilation probability and leading to a larger fraction of delayed fluorescence. Details on these scintillation mechanisms can be found in text books [13] and review articles [14].

This scenario is the basis of the "highly concentrated primary fluorophore" strategy that various groups have studied [10]. This strategy requires performing molecular design to tune the photophysical properties of the "primary scintillating fluorophore". Typically, the fluorophore must absorb in the wavelength range from 260 to 340 nm and emit in the wavelength range from 330 to 380 nm, so that the emitted photons can be absorbed and re-emitted by a secondary fluorophore. Obviously, the photoluminescence quantum yield must be as high as possible. Furthermore, since high concentrations are required (typically 15 to 40 wt% in polystyrene or poly(vinyltoluene)), this molecule must be highly soluble in apolar solvents and must not be exuded from the polymer with time. Currently only a few molecules fulfil all these criteria: 2,5-diphenyloxazole (PPO) and derivatives [15], biphenyl [16], various oxadiazole derivatives [17], non-commercial terphenyl- and fluorene-based fluorophores [18], with PPO being the most widely used primary fluorophore. Recently, developments in polysiloxane-based scintillators have highlighted a neutron detection efficiency with materials loaded with lower concentrations [19].

After a thorough work dedicated to chemical optimization and material stability, several studies have also been performed towards a detection system: radiation damage studies [20], coupling of these scintillators to silicon photomultipliers [21], dedicated algorithms [22] and neutron imaging [23]. Currently, one of the major concerns is the increase of the size of the scintillators since radiation portal monitors usually require monoliths with a volume larger than 10 L. In this context, it is shown that the fast neutron/gamma discrimination ability of plastic scintillators decreases faster with dimensions than that of their liquids counterparts [15], [24]. Self-absorption of the scintillation light might be one of the main causes of this decrease [25], and is one of the motivations of the present work. Since the transition from the time scales dominated by fast fluorescence to the time region of the sole delayed fluorescence occurs for times of a few tens of ns, it is assumed that multiple absorption–reemission processes might stretch this transition region, thus leading to a partial confusion of the two components and to the degradation of the PSD performance with the photon path length. In this context, we describe here our latest investigation with 1-phenyl-3-(mesityl)-2-pyrazoline (**1**) as a unique fluorophore for fast neutron/gamma discrimination.

Compound **1** was originally synthesized and tested in scintillation counting by Güsten et al. some decades ago [26]. This compound has the unusual feature of being an efficient highly soluble fluorophore with large Stokes shift (68,490 cm^{-1} according to our experimental spectra-vide infra) resulting in a quasi-negligible overlap of emission and absorption spectra. This property allows the design of liquid or solid scintillators and even scintillating fibres with compound **1** as primary solute without requiring a wavelength shifter like the widely used 1,4-bis(5-phenyloxazol-2-yl) benzene (POPOP). Despite all these claimed qualities and possible modification of its core structure [27], to the best of our knowledge, compound **1** remains surprisingly unused as a suitable fluorophore for n/γ discriminating plastics. Since self-absorption might be a limitation to n/γ PSD, the use of fluorophores with important Stokes shift could be a breakthrough towards large-volume materials. However, the

high concentration strategy obviously requires large quantities of the fluorophore, and compound **1** is not readily available.

Here, we report the original use of compound **1** (Fig. 1) at high concentration in poly(vinyltoluene) matrices for neutron/gamma discrimination by PSD technique. A large-scale synthesis is described first, then compound **1** based scintillators are prepared and characterized.

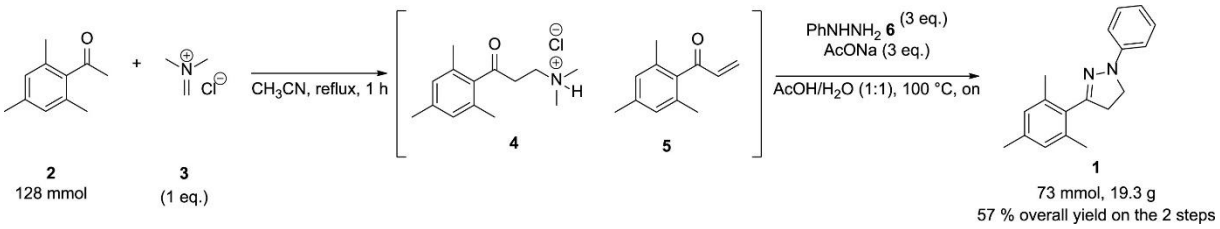

Fig. 1. Synthesis of 1-phenyl-3-(mesityl)-2-pyrazoline (**1**). Noteworthy is that this two-step reaction strategy proceeded smoothly when applied to the large-scale synthesis of **1** starting from 128 mmol of **2** to afford 19.3 g of pure compound **1**.

2. Results and discussion

Compound **1** is commercially available from only few suppliers and due to its price and the quantity required for large concentration loading in plastics, we firstly envisaged to reinvestigate its synthesis on large scale. The synthesis of compound **1** was shortly depicted in the literature by Güsten and co-workers who obtained compound **1** by condensation of mesitylvinylketone and phenylhydrazine [26]. However, synthesis of its analogue with a phenyl group on the C3-position instead of mesityl offered more synthetic strategies. One straightforward strategy involves a Mannich reaction [28] with the commercially available mesitylacetophenone **2** [29] and Eschenmoser's salt [30] **3** and attracted our attention as the starting material is less expensive than mesitylphenylketone which is necessary in Güsten strategy (Fig. 1). In our first attempt to isolate the Mannich product, ^{1}H NMR spectroscopy showed that a 4:1 ratio between the ammonium **4** resulting from the Mannich reaction and the α,β-unsaturated ketone **5** was obtained. Indeed, when compound **4** is formed, an elimination of the dimethylammonium framework occurs, resulting in the formation of **5**. Nevertheless, as compound **5** is the starting material of the Güsten strategy, a sequential reaction without purification was envisaged [31]. The crude Mannich reaction was directly engaged in the cyclization with phenylhydrazine **6** leading to compound **1**. As the purity of the compound **1** is mandatory for the preparation of plastics, the chromatographied compound **1** was also recrystallized in methanol and isolated within 57% isolated overall yield for two steps. Once the synthesis of compound **1** was achieved, we turned our attention to the choice of the matrix for our future plastic. To optimize the energy transfer from the matrix to compound **1**, emission spectra of the matrix and absorption of the fluorophore should overlap each other in order to facilitate Förster Resonance Energy Transfer (FRET) between matrix and compound **1**. Another advantage for such selection and related to energy transfer is the presence of aromatic rings in both compound **1** and PVT which might create π-π interactions allowing electron exchange by Dexter mechanism. Considering this point, polyvinyltoluene (PVT) appeared to be a good candidate with the additional advantage of being readily prepared from a low-cost monomer. Additionally, PVT is the matrix material of the commercially produced EJ-200 that can be used as standard for comparison of the PSD properties. In order to show the good overlap of PVT emission and absorption of compound **1**, absorption and emission spectra were recorded for PVT using shavings from a plastic prepared with pure vinyltoluene in our general conditions and our prepared compound **1** dissolved in dichloromethane at concentrations of 2.5×10^{-3} gL^{-1} and 10^{-4} mol L^{-1}, respectively. The results are presented in Fig. 2.

Absorption of PVT (Fig. 2) exhibits several maxima in the UV region and notably between 230 to 275 nm) assigned to $\pi \rightarrow \pi^*$ transitions of PVT. Emission of PVT (Fig. 2), also located in UV region, presents a broadened band between 290 to 375 nm.

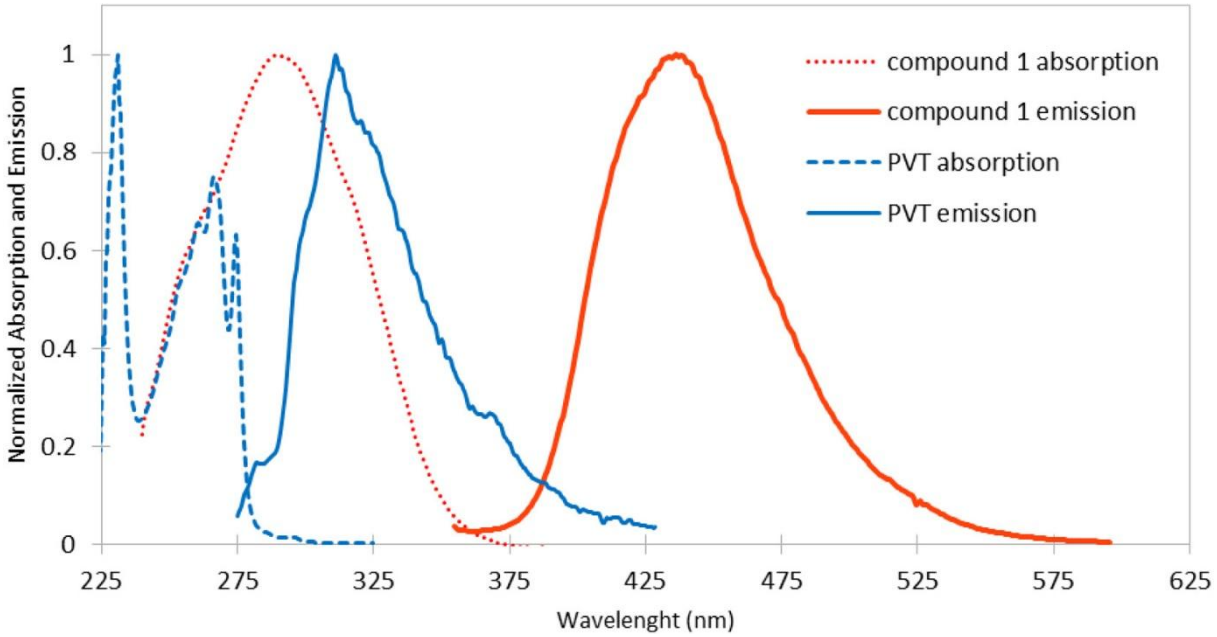

Fig. 2. Normalized UV–visible spectra of PVT (PVT from a sample of pure vinyltoluene polymerized following our general condition and dissolved in dichloromethane, C = 2.5×10^{-3} mg mL^{-1}) (blue dashed line) and compound **1** (in dichloromethane C = 10^{-4} mol L^{-1}, red dotted line) and, normalized fluorescence spectra of PVT (solid state in front face conditions, excitation at 275 nm) (blue full line) and compound **1** (solution in dichloromethane, C = 10^{-4} mol L^{-1}, excitation at 295 nm) (red full line).

This latter overlaps the absorption of compound **1** which covers the UV region between 225 to 350 nm. This absorption is also assigned to $\pi \rightarrow \pi^*$ transitions. Finally, the emission spectrum of compound **1** exhibits a maximum centred at 425 nm corresponding to the violet region adapted to our future setup for radioluminescence measurements, which uses a photomultiplier tube. Plastics composed by PVT and compound **1** were prepared on a 10 g scale with concentrations of compound **1** of 0, 1, 2, 3, 4, 5, 10, 15, 20, 25 and 30 wt%. Vinyltoluene was freshly distilled and degassed by the *freeze-pump-thaw* technique five times.

After preparation of the vinyltoluene and compound **1** mixture under argon atmosphere in previously silanized vial, sonication of the mixture was achieved to homogenize the solution. Vials were then placed in an oven at 120 °C for 5 days before letting vials slowly cool down to room temperature (no initiator was required for the polymerization of the vinyltoluene). The resulting plastic was then removed from the vial and polished.

Increasing the fluorophore doping in the polymer matrix might lead to a decrease of the physical hardness of the plastic matrix [32]. Once our compound **1** doped plastics were obtained, their hardness was determined using a Shore-D durometer. The values obtained for these plastics are reported in Table 1 and shown on Fig. 3 as a function of the concentration of compound **1**.

For concentrations of compound **1** between 1 to 25 wt%, the hardnesses were found to be similar and varied between 81 and 86 Shore-D. These values correspond to the hardness measured for a pure PVT plastic (i.e. 0 wt% of **1**). This is also the value usually observed for commercial plastics such as BC-408 [33] (Shore-D = 85), BC-428 (Shore-D = 88) or EJ-226 [34] (Shore-D = 89). A dramatic decrease of the hardness to 62 Shore-D was observed at a high concentration of 30 wt% of compound **1** (Table 1 and Fig. 3).

[1] wt%[a]		**0**	**1**	**2**	**3**	**4**	**5**	**10**	**15**	**20**	**25**	**30**
Hardness (Shore-D)		82	83	81	81	81	85	86	83	84	83	62
Average molecular weight of PVT ($\times 10^3$ g mol^{-1})	M_w M_n	335 122	N.D.[b] N.D.[b]	N.D.[b] N.D.[b]	N.D.[b] N.D.[b]	N.D.[b] N.D.[b]	286 112	237 95	220 92	186 78	166 70	151 69
Dispersity	D_M	2.73	N.D.[b]	N.D.[b]	N.D.[b]	N.D.[b]	2.56	2.50	2.40	2.39	2.36	2.18

Table 1. Hardness, weight average molecular weight M_w, number average molecular weight M_n and dispersity of plastic scintillators containing compound **1**.

[a] wt% of compound **1** in the PVT matrix.

[b] N.D. Not determined.

This critical concentration of compound **1** could also have impact on the characteristics of polymer, *e.g.* the length of PVT chains. To confirm this hypothesis, size exclusion chromatography (SEC) in dichloromethane was performed on plastic samples with concentrations of compound **1** from 0 to 30 wt%. Results are summarized in Table 1 and Fig. 3 for better comparison with the physical hardness of the plastic scintillators. One can notice that the weight average molecular weight (M_w) and the number average molecular weight (M_n) of the PVT decrease with the increase in dopant concentration (compound **1**). In particular, M_w drops from 335 to 151 × 10^3 g mol^{-1} when the concentration increases from 0 to 30 wt% (Table 1). In conclusion, our plastics keep an acceptable hardness until a concentration of compound **1** of 25 wt%, for which the PVT matrix has a weight average molecular weight M_w of 166 × 10^3 g mol^{-1} (Table 1). This high concentration of compound **1** impacts the average molecular weight M_w of the final PVT but its role during the polymerization of vinyltoluene remains unclear.

To control the presence of compound **1** during the polymerization of vinyltoluene in plastic preparation, two 1 g PVT plastic samples were produced following the same procedure as for the 10 g plastics with 0 and 5 wt% of compound **1**. These plastics were then ground and studied with Fourier-transform infrared spectroscopy together with a sample of pure compound **1** (crystals obtained after purification and ground into powder) (Figure S1 in ESI).

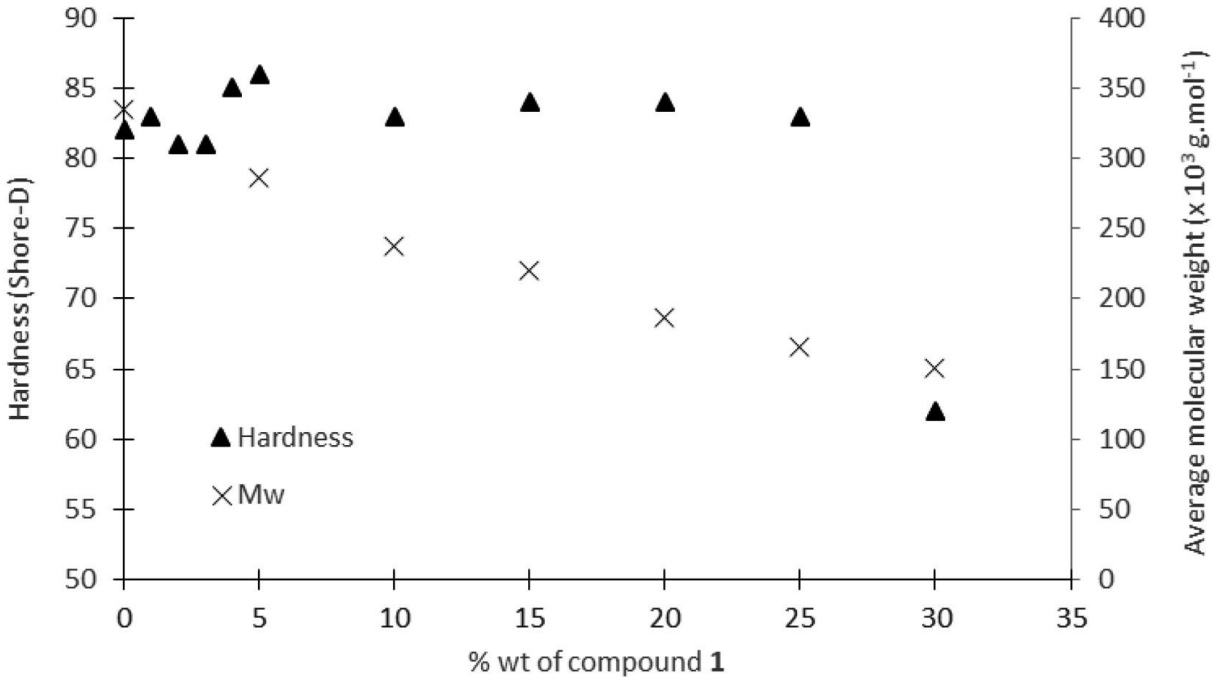

Fig. 3. Hardness (Shore-D) (bold triangles) and weight average molecular weight (M_w dark crosses) of PVT (g mol^{-1}) of plastic scintillators as a function of compound **1** concentration (wt%).

The band at wavelength number of 1600 cm^{-1} was selected as reference of compound **1**, as in the infrared spectrum of the pure PVT plastic no band appeared in this region. This band at 1600 cm^{-1}, assigned to the C=N bond stretching in compound **1**, was detected in the infrared spectrum of the ground PVT plastic containing 5 wt% of compound **1**, confirming the presence of compound **1** after polymerization.

To quantify compound **1** in our sample, a thermogravimetric analysis (TGA) was performed on the same samples, *i.e.* the pure PVT plastic, pure compound **1** and the plastic containing 5 wt% of compound **1**.

TGA of the pure PVT plastic shows a slight drop of weight when the temperature increases from 150 to 200 °C, probably due to the presence of residual monomer in the plastic (boiling point of vinyltoluene is 170 °C). Then a 99.8% drop of mass was observed for a temperature varying between 412.8 °C and 454.5 °C (Fig. 4). TGA of compound **1** exhibits a 99.8% drop of mass as temperature varies from 293.3 to 343.3 °C (Fig. 4). Finally, TGA of the PVT plastic containing 5 wt% of compound **1** shows the same slight drop of mass as for the pure PVT sample when the temperature increases from 150 to 200 °C (Fig. 4). A total loss of mass of 8.2% can be quantified when temperature reaches 343.3 °C. As compound **1** was introduced at 5 wt%, the residual vinyltoluene monomer can be reasonably considered at around 3 % in the plastic. A final drop of mass of about 91.8% is measured when temperature reaches 454.5 °C, corresponding to the PVT.

As the sample shape is important for the determination of the light output (LO) and PSD properties, plastics were all prepared as Ø 28 mm × 14 mm cylinders. To evaluate the LO of our plastics containing 5, 10, 15, 20, 25, and 30 wt% of compound **1**, polished samples were put in the presence of a ^{137}Cs gamma source. To determine their LO, our plastics were compared to a sample of EJ-200 commercial plastic scintillator machined to a similar shape as our samples. Relative LO of plastics containing 5, 10, 15, 20, 25 and 30 wt% of compound **1** are reported in Table 2 and Fig. 5.

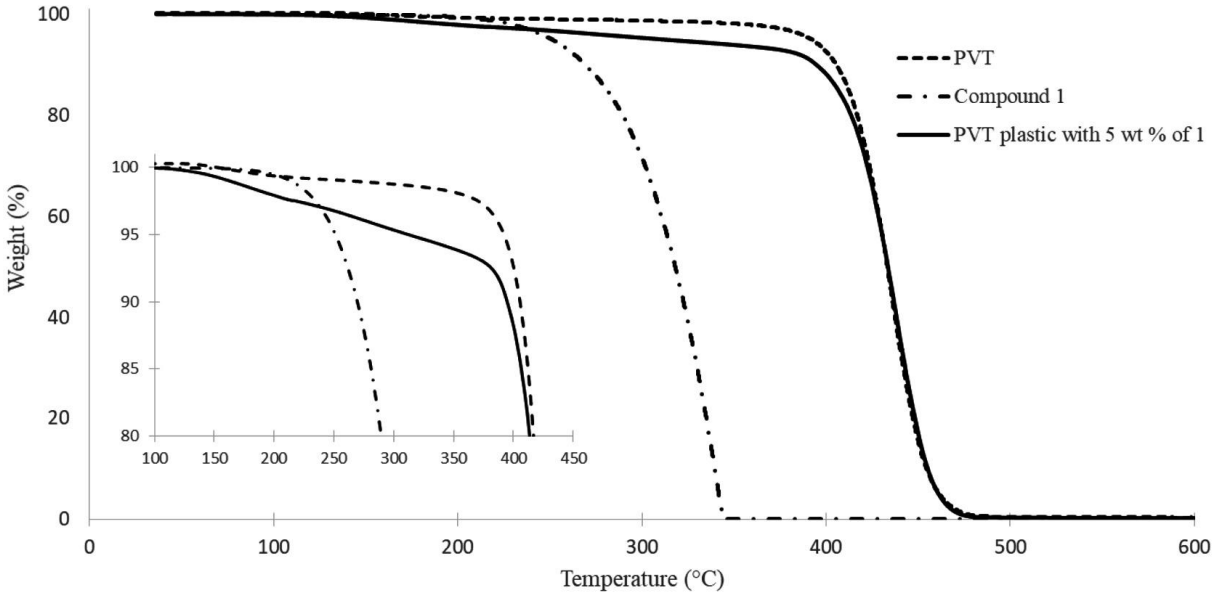

Fig. 4. TGA of pure PVT plastic, compound **1** and PVT plastic containing 5 wt% of compound **1** (inset in the range of temperature of 100 to 450 °C with a loss of weight of 20% maximum).

Relative LO of plastics were found to decrease from 0.74 to 0.32 (LO of EJ-200 being set to 1) with the increase of the concentration of compound **1** from 5 to 30 wt%. Such trend has also been observed with PPO as a single fluorophore in plastic scintillator [11].

Doping of 1 in PVT plastic (wt%)	LO[a] (%)	t_{slow}[b] (ns)	FoM[c]
5	0.74	40	0.52
10	0.65	40	0.68
15	0.65	30	0.84
20	0.45	25	0.74
25	0.35	25	0.65
30	0.32	25	0.63

Table 2. Scintillation and discrimination properties of plastics containing different concentrations of compound **1**.

[a] Relative LO compared to the LO of a EJ-200 sample with the same shape as our plastics doped with compound **1**.

[b] Optimal start time of the delayed integration window, given with respect to the time of the pulse maximum.

[c] Discrimination figure of merit (FoM) measured for a total light in the range 450–500 keVee.

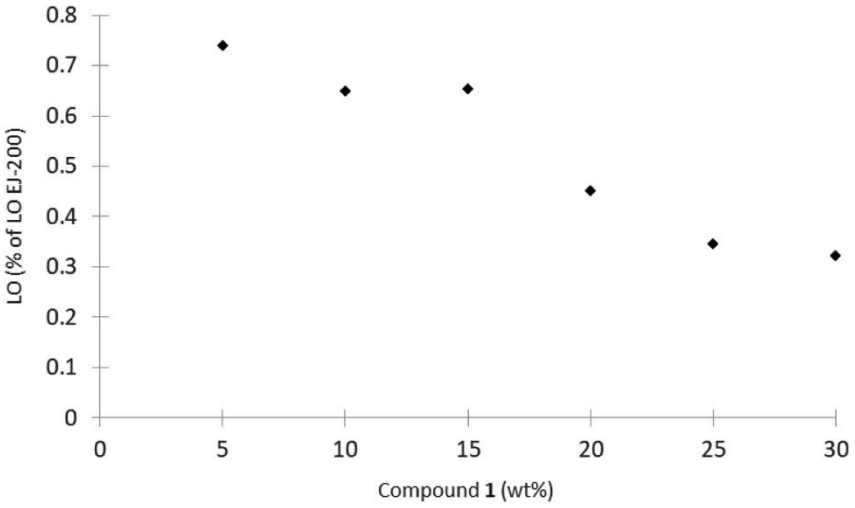

Fig. 5. LO (relative to LO of an EJ-200 sample) of PVT plastics incorporating 5, 10, 15, 20, 25, 30 wt% of compound **1**.

The neutron/gamma discrimination capability of the plastic samples was investigated next.

All samples were alternatively coupled to the same Hamamatsu R329-02 photomultiplier tube (diameter 5 cm) equipped with the same voltage divider (assembly H7195), in order to avoid variations from physically different photomultiplier tubes. To limit gain and response fluctuations, the same high voltage was applied to the photomultiplier tube for all samples.

Measurements were performed with the samples exposed to an AmBe neutron and gamma-ray source and the FASTER digital electronics and data acquisition system [35]. Discrimination was performed using the charge integration method [36] which is based on the integration of the scintillation light over two time windows, one covering the full signal to give the total light L_{tot}t, and the other one set on the pulse tail to integrate the delayed light L_{slow}. The fraction of delayed light L_{slow}/L_{tot} was taken as the discriminating variable. The time window used to integrate the total light L_{tot} started 20 ns before the time of the pulse maximum, the rise time of the pulse being about 10 ns. While increasing the duration of this window was found to lead to a higher discrimination quality, it was limited to 600 ns in order to match the duration of operation of the digital baseline restoration algorithm. The start time of the delayed window used for L_{slow} integration was varied for each sample independently to search for the best discrimination quality. The optimal start time is reported in Table 2 for each sample. It is given with respect to the time of the pulse maximum. The delayed integration window ended at the same time as the L_{tot} window. Using a ^{22}Na source, L_{tot} was calibrated in keVee (keV electron equivalent),

i.e. in terms of the light produced by the deposition of a given electron energy. More precisely, the raw L_{tot} values taken at 50% of the heights of the Compton edges of the 511 and 1275-keV gamma-rays of ^{22}Na were associated to the corresponding maximum Compton electron energies. Such a choice is often made for the light calibration of organic scintillators [37], and is expected to be a good approximation in our case of samples with a small size. Indeed, previous systematic studies showed that the difference between the light corresponding to the Compton edge energy and that corresponding to 50% of the maximum number of counts in the Compton edge region decreases as the size of the scintillator decreases [38], and is of the order of a few % for scintillators with a volume five times larger than our sample volume. Therefore, this difference should even be smaller for our relatively small samples. As the response of organic scintillators is linear for electron energies above some 100 keV, a linear light to energy relation was assumed. Neutron/gamma discrimination was possible with all samples. This is illustrated on Fig. 6 which shows the ratio as a function of L_{slow}/L_{tot} for the plastics doped with 5, 15 and 30 wt % of compound **1**.

On each plot, two groups can be distinguished, one at a larger L_{slow}/L_{tot} ratio corresponding to neutrons and another one at smaller L_{slow}/L_{tot} containing gamma-ray interactions. For comparison purposes, the discrimination quality was measured for L_{tot} in the range 450–500 keVee by the "figure of merit" (FoM) defined as the ratio of the separation S between the average neutron and gamma-ray L_{slow}/L_{tot} and the sum of the full widths at half maximum of the two distributions, W_n and W_{gamma}, FoM $=S / (W_n + W_{gamma})$, as illustrated on Fig. 7. The FoM values measured for L_{tot} in the range 450–500 keVee with the different samples are given in Table 2 and shown on Fig. 8 as a function of the concentration of compound **1**. Uncertainties on these values are 0.02. The best FoM in the range 450–500 keVee was determined to be 0.84 with the plastic doped with 15 wt% of compound **1**.

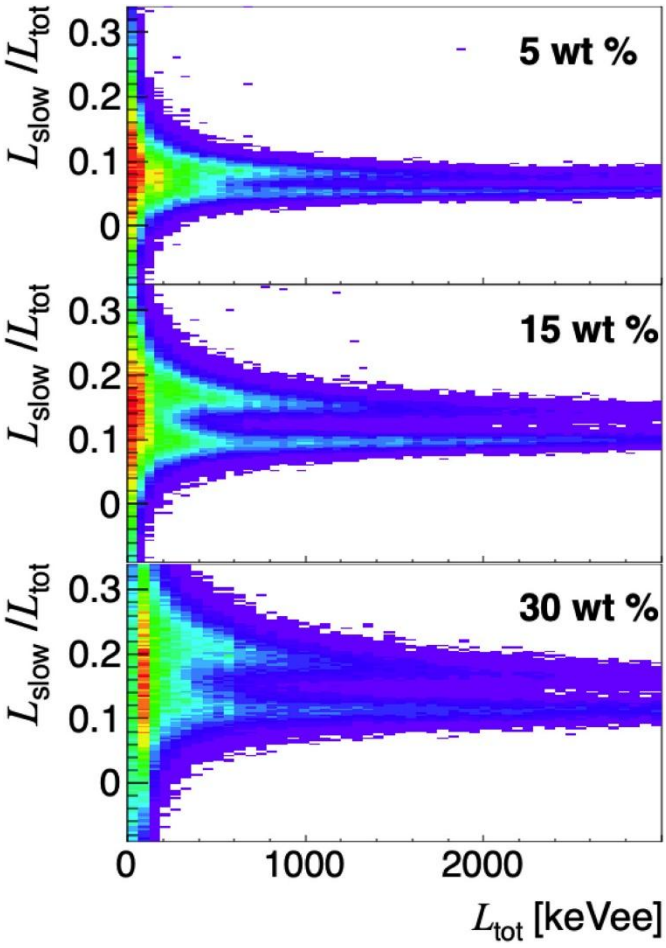

Fig. 6. Discrimination plots for the plastic samples doped with 5 wt% (upper panel), 15 wt% (central panel) and 30 wt% (lower panel) of compound **1**.

Our measurement with a Ø 50 mm × 50 mm cylindrical cell of the BC-501 A liquid scintillator using the same setup and experimental procedure leads to a FoM value of 1.99 in the range 450–500 keVee. However, we note that for a FoM value of 0.80, the fraction of misidentified neutrons or gamma-rays is typically of the order of 3–4 %. This already corresponds to a reasonably good discrimination.

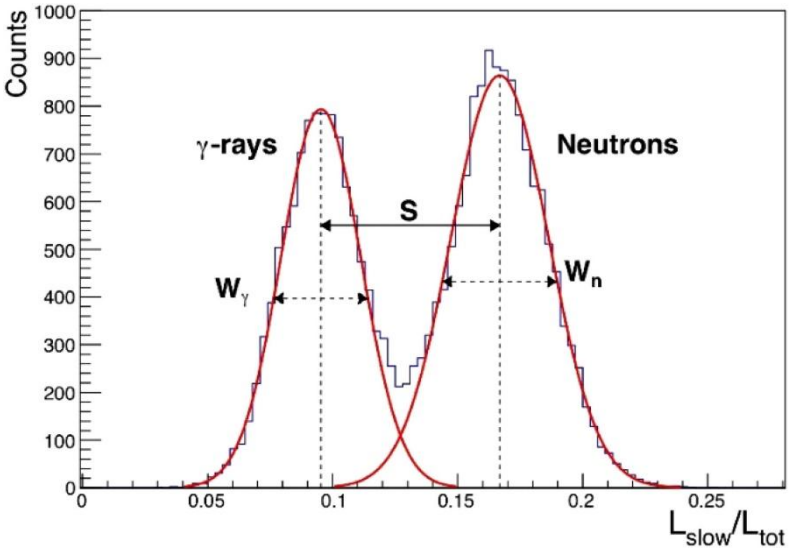

Fig. 7. Distribution of the discriminating variable L_{slow}/L_{tot} for L_{tot} in the range 450–500 keVee for the plastic sample doped with 15 wt% of compound **1**.

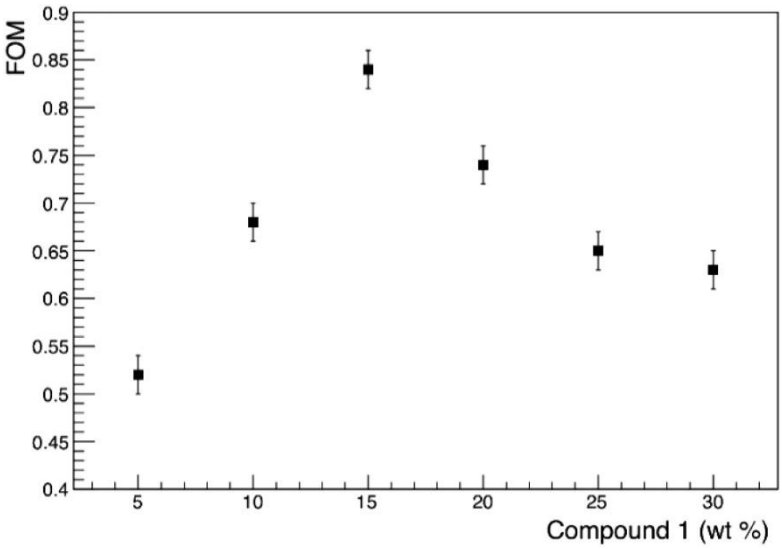

Fig. 8. Discrimination figures of merit (FoM) of the PVT plastics incorporating 5–30 wt% of compound **1**, measured in the range 450–500 keVee.

Comparing Fig. 5, Fig. 8, one can notice that at the compound **1** concentration optimum for PSD (15 wt%), the light output is reduced with respect to that obtained at lower concentration. This is similar to previous observations with PVT plastics loaded with PPO [11].

If we compare now the performance of our plastic containing 15 wt% of compound **1** with the commercially available EJ-276, the FoM of our scintillator is 0.84 vs. 2.8 for EJ-276 [39], and its light output is 0.65 vs. 0.84 for EJ-276. While fresh EJ-276 exhibits higher performance than our plastic scintillators, some drawbacks of this commercially available scintillator can be mentioned. Indeed, the addition of a secondary dye is necessary to reach the same Stokes shift as in our plastic scintillator using compound **1** as sole fluorophore. Then, EJ-276 is an oxygen-sensitive material leading to a loss of around 20 % per year of its FoM [40], thus requiring this product to be sold encapsulated in an aluminum housing. But here we do not claim to have in hand a commercial product.

3. Conclusion

In conclusion, we have performed a new robust and multi-gram scale (nearly 20 g, 73 mmol) synthesis of compound **1** from low-cost chemicals (price of compound **1** is 459 € for 5 g, representing 18.9 mmol vs. price of the mesitylmethylketone, 841 € for 500 g, representing 3082 mmol; other starting chemicals have a negligible cost) [41]. The synthesis of a high amount of this blue-emitting organic compound allowed us to prepare a series of PVT-based plastics. These plastics doped with a sole fluorophore exhibit good LO when exposed to ionizing radiation and were found able to discriminate fast neutrons from gamma-rays. The highest discrimination quality was obtained with a doping concentration of compound **1** of 15 wt%. The polymer characterization on the plastic matrix has shown that the hardness of the plastic dramatically decreases with a high fluorophore concentration of 30 wt%. It appears that increasing the concentration of primary fluorophore leads to a decrease of the molecular weight. This relationship between molecular weight and primary fluorophore concentration is to our knowledge the first of its kind. Further investigations are ongoing in our laboratories to understand the mechanism of the PSD with our plastics containing compound **1** as primary fluorophore.

CRediT authorship contribution statement

Fabrice Bisaro: Investigation, Methodology, Writing – original draft.
Alya Inial: Investigation, Methodology.
Jérémie Gatignol: Investigation, Methodology.
Florent Allix: Investigation, Methodology.
Aurélie Stallivieri: Investigation, Methodology.
Jean-Luc Renaud: Investigation, Writing – original draft.
Lynda Achouri: Investigation.
Marian Parlog: Investigation.
Franck Delaunay: Investigation, Writing – original draft.
Thi-Nhàn Pham: Funding acquisition, Validation.
Matthieu Hamel: Conceptualization, Funding acquisition, Project administration, Supervision, Validation, Writing – original draft.
Sylvain Gaillard: Conceptualization, Funding acquisition, Project administration, Supervision, Validation, Writing – original draft.

Declaration of Competing Interest

The authors declare that they have no known competing financial interests or personal relationships that could have appeared to influence the work reported in this paper.

Acknowledgements

Funding

The authors are indebted to the “Agence Nationale de la Recherche”, France for the grant allowed to the Nessyned project [ANR-15-CE39-0006]. SG thanks the region Normandie for co-funding the Nessyned project. This work was also supported by the “Ministère de la Recherche et des Nouvelles Technologies” and the CNRS (Centre National de la Recherche Scientifique), France.

Appendix A. Supplementary data

The following is the Supplementary material related to this article.

References

[1] Fraboni B., Fraleoni-Morgera A., Zaitseva N. - Adv. Funct. Mater., 26 (2016), pp. 2276-2291

[2] Salonen L., Kaihola L., Carter B., Cook G.T., Passo C.J. Jr. - L'Annunziata M.F. (Ed.), Handbook of Radioactivity Analysis (third ed.), Academic Press (2012), pp. 625-693

[3] Bertrand G.H.V., Hamel M., Sguerra F. Chem. - Eur. J., 20 (2014), pp. 15660-15685

[4] Carlson J.S., Marleau P., Zarkesh R.A., Feng P.L. - J. Am. Chem. Soc., 139 (2017), pp. 9621-9626

[5] Dujardin C., Auffray E., Bourret-Courchesne E., Dorenbos P., Lecoq P., Nikl M., Vasil'ev A.N., Yoshikawa A., Zhu R.-Y.- IEEE Trans. Nucl. Sci., 65 (2018), pp. 1977-1997

[6] Lewis J.M., Kelley R.P., Murer D., Jordan K.A. - Appl. Phys. Lett., 105 (2014), Article 014102

[7] Peerani P., Tomanin A., Pozzi S., Dolan J., Miller E., Flaska M., Battaglieri M., De Vita R., Ficini L., Ottonello G., Ricco G., Dermody G., Giles C. - Nucl. Instrum. Methods A, 696 (2012), pp. 110-120

[8] (a) Nemchenok I.B., Babin V.I., Brudanin V.B., Kochetov O.I., Timkin V.V. - Phys. Part. Nucl. Lett., 8 (2011), pp. 129-135

(b) Ye X.-C., Yu B.-X., Zhou X., Zhao L., Ding Y.-Y., Liu M.-C., Ding X.-F., Zhang X., Jie Q.-L., Zhou L., Fang J., Chen H.-T., Hu W., Niu S.-L., Yan J.-Q., Zhao H., Hong D.-J. - Chin. Phys. C, 39 (2015), p. 096003

(c) Janda J. - J. Lumin., 230 (2021), p. 117714

[9] (a) Neumann K.E., Roessier N., ter Wiel J. - Ross H., Noakes J.E., Spauling J.D. (Eds.), Liquid Scintillation Counting and Organic Scintillators, Lewis, Chelsea, MI (1991), pp. 35-41

(b) Feng X.-G., He Q.-G., Wang J.-C., Chen J. Appl. Radiat. Isot., 70 (2012), p. 1536-1540

[10] Brooks F.D., Pringle R.W., Funt B.L. - IRE Trans. Nucl. Sci., NS-7 (1960), pp. 35-38

[11] Zaitseva N., Rupert B.L., Pawełczak I., Glenn A., Martinez H.P., Carman L., Faust M., Cherepy N., Payne S. - Nucl. Instrum. Methods A, 668 (2012), pp. 88-93

[12] (a) Hajagos T.J., Liu C., Cherepy N.J., Pei Q. - Adv. Mater., 30 (2018), Article 1706956

(b) Tarancón A., Bagán H., García J.F. - J. Radioanal. Nucl. Chem., 314 (2017), p. 555-572

(c) Beaulieu L., beddar S. - Phys. Med. Biol., 61 (2016), p. R305-R343

(d) Bertrand G.H.V., Hamel M., Normand S., Sguerra F. - Nucl. Instrum. Methods A, 776 (2015), p. 114-128

[13] (a) Birks J.B. - The Theory and Practice of Scintillation Counting, Pergamon Press, London (1964)

(b) Knoll G.F. - Radiation Detection and Measurements (third ed.), John Wiley and Sons, New York (2000)

[14] Brooks F.D. - Nucl. Instrum. Methods, 162 (1979), pp. 477-505

[15] (a) N. P. Zaitseva F.D., Glenn A.M., Mabe A.N., Carman M.L., Hurlbut C.R., Inman J.W., Payne S.A. - Nucl. Instrum. Methods A, 889 (2018), pp. 97-104

(b) Zhmurin P.N., Eliseev D.A., Pereymak V.N., Svidlo O.V., Gurkalenko Y.A. - Funct. Mater., 24 (2017), p. 476-480

(c) van Loef E., Markosyan G., Shirwadkar U., McClish M., Shah K. - Nucl. Instrum. Methods A, 788 (2015), p. 71-72

[16] Blanc P., Hamel M., Dehé-Pittance C., Rocha L., Pansu R.B., Normand S. - Nucl. Instrum. Methods A, 750 (2014), pp. 1-11

[17] Zhmurin P. - Engineering of Scintillation Materials and Radiation Technologies, Proceedings of ISMART 2016, Publishing, S. I. Ed, Cham (2017), pp. 129-149

[18] Yemam H.A., Mahl A., Tinkhan J.S., Koubek J.T., Greife U., Sellinger A. - Chem. - Eur. J., 23 (2017), pp. 8921-8931

[19] (a) Marchi T., Pino F., Fontana C.L., Quaranta A., Zanazzi E., Vesco M., Cinausero M., Daldosso N., Paterlini V., Gramegna F., Moretto S., Collazuol G., Degerlier M., Fabris D., Carturan S.M. - Sci. Rep., 9 (2019), p. 9154

(b) Lim A., Arrue J., Rose P.B., Sellinger A., Erickson A.S. - ACS Appl. Polym. Mater., 2 (2020), p. 3657-3662

[20] Montbarbon E., Amiot M.-N., Tromson D., Gaillard S., Frangville C., Woo R., Bertrand G.H.V., Pansu R.B., Renaud J.-L., Hamel M. - Phys. Chem. Chem. Phys., 19 (2017), pp. 28105-28115

[21] (a) Taggart M.P., Sellin P.J. - Nucl. Instrum. Methods A, 908 (2018), pp. 148-154

(b) Yu J., Wei Z., Fang M., Zhang Z., Cheng C., Wang Y., Su H., Ran Y., Zhu Q., Zhang H., Duan K., Chen M., Liu M.- Nucl. Instrum. Methods A, 894 (2018), p. 129-137

(c) Grodzicka-Kobylka M., Szczesniak T., Moszyński M., Swiderski L., Wolski D., Baszak J., Korolczuk S., Schotanus P. - Nucl. Instrum. Methods A, 883 (2018), p. 159-165

[22] (a) French R.M., Thevenin M., Hamel M., Montbarbon E. IEEE Trans. Nucl. Sci., 64 (2017), pp. 2423-2432

(b) Langeveld W.G.J., King M.J., Kwong J., Wakeford D.T. - IEEE Trans. Nucl. Sci., 64 (2017), p. 1801-1809

(c) Prusachenko P.S., Khryachkov V.A., Ketlerov V.V., Bokhovko M.V., Bondarenko I.P. - Nucl. Instrum. Methods A, 905 (2018), p. 160-170

[23] Chuirazzi W.C., Oksuz I., Kandlakunta P., Massey T.N., Brune C.R., Cherepy N.J., Martinez H.P., Cao L.J. - J. Radioanal. Nucl. Chem., 318 (2018), pp. 543-551

[24] Grodzicka-Kobylka M., Szczesniak T., Moszynski M., Brylew K., Swiderski L., Valiente-Dobón J.J., Schotanus P., Grodzicki K., Trzaskowska H. - J. Instrum., 15 (2020), p. P03030

[25] Montbarbon E., Zhang Z., Grabowski A., Woo R., Tromson D., Dehé-Pittance C., Pansu R.B., Bertrand G.H.V., Hamel M. - J. Lumin., 213 (2019), pp. 67-74

[26] (a) Güsten H., Schuster P., Seitz W. - J. Phys. Chem., 82 (1978), pp. 459-463

(b) Janda J., Rajchl E. - J. Radioanal. Nucl. Chem., 318 (2018), p. 2235-2245

(c) Janda J., Rajchl E. - J. Lumin., 201 (2018), p. 390-396

[27] Bliznyuk V.N., Seliman A.F., Ishchenko A.A., Derevyanko N.A., DeVol T.A. - ACS Appl. Mater. Interfaces, 8 (2016), pp. 12843-12851

[28] (a) Jacob A., Madinaveitia J. - J. Chem. Soc., 0 (1937), pp. 1929-1931

(b) Nisbet H.B. - J. Chem. Soc. (1945), p. 126-129

(c) G.F. Duffin, J.D. Kendall - 1953, US Patent 2, 640, 056.

(d) Duffin G.F., Kendall J.D. - J. Chem. Soc. (1954), p. 408-411

(e) Duffin G.F., Kendall J.D. - J. Chem. Soc. (1955), p. 3470-3474

(f) Abid M., Azam A. - Bioorg. Med. Chem., 13 (2005), p. 2213-2220

(g) Karakus C., Fischer L.H., Schmeding S., Hummel J., Risch N., Schäferling M, Holder E. - Dalton Trans., 41 (2012), p. 9623-9632

[29] (a) Mesitylketone derivatives can also be prepared by Friedel-Crafts reaction starting from 420 mesitylene and acid chlorides, see:

Zhou Y., Li X., Hou S., Xu J. - J. Mol. Catal. A: Chem., 365 (2012), pp. 203-211

(b) Mehdi K.M., Kiumars B., Fomeida S. - Chem. Lett., 37 (2008), p. 844-845

[30] Schreiber J., Maag H., Hashimoto N., Eschenmoser A.E. - Angew. Chem. Int. Ed. Engl., 10 (1971), pp. 330-331

[31] Wagner A., Schellhammer C.-W., Petersen S. - Angew. Chem. Int. Ed. Eng., 5 (1966), pp. 699-704

[32] For a publication mentioning plastic deformation and physical hardness, see: a) ref 15a. b) A. Lim, G. Hernandez, J. Latta, H. A. Yemam, W. Senevirathna, U. Greife, A. Sellinger, ACS Appl. Polym. Mater. 1 (2019), 1420-1429.

[33] Mahl A., Lim A., Latta J., Yemam H.A., Greife U., Sellinger A. - Nucl. Instrum. Methods A, 884 (2018), pp. 113-118

[34] Hamel M., Pjatkan R., Burešová H. - Nucl. Instrum. Methods A, 955 (2020), Article 163294

[35] http://faster.in2p3.fr/.

[36] Heltsley J.H., Brandon L., Galonsky A., Heilbronn L., Remington B.A., Langer S., Vander Molen A., Yurkon J., Kasagi J. - Nucl. Instrum. Methods A, 263 (1988), pp. 441-445

[37] Pagano E.V., Chatterjee M.B., De Filippo E., Russotto P., Auditore L., Cardella G., Geraci E., Gnoffo B., Guazzoni C., Lanzalone G., De Luca S., Maiolino C., Martorana N.S., Pagano A., Papa M., Parsani T., Pirrone S., Politi G., Porto F., Quattrocchi L., Rizzo F., Trifirò A., Trimarchi M. - Nucl. Instrum. Methods A, 889 (2018), pp. 83-88

[38] Zaitseva N.P., Glenn A.M., Carman M.L., Mabe A.N., Payne S.A., Marom N., Wang X. - Nucl. Instrum. Methods A, 978 (2020), Article 164455

[39] Dietze G., Klein H. - Nucl. Instrum. Methods, 193 (1982), pp. 549-556

[40] Zaitseva N.P., Carman M.L., Glenn A.M., A. N. Mabe A.N. - Neutron/gamma pulse shape discrimination in plastics scintillators: from development to commercialization. Hamel M. (Ed.), Plastic Scintillators: Chemistry and Applications, Topics in Applied Physics, vol. 140, Springer, Cham (2021)

[41] a) Price for compound 1 was found on TCI® website, https://www.tcichemicals.com/FR/en/p/P1951 (the 26th of 2021),

b) Price for mesitylmethylketone was found on Thermofisher® website https://www.alfa.com/fr/catalog/A11549/ (the 26th of 2021).